Available online at www.sciencedirect.com
ScienceDirect
Aerosol Science 37 (2006) 1717–1729
Journal of Aerosol Science
www.elsevier.com/locate/jaerosci

Analytic and numerical calculations of the formation of a sulphuric acid aerosol in the upper troposphere

C.F. Clement[a], L. Pirjola[b,c], C.H. Twohy[d], I.J. Ford[e,*], M. Kulmala[b]

[a] *15 Witan Way, Wantage, Oxfordshire OX12 9EU, UK*
[b] *Department of Physical Sciences, University of Helsinki, P.O. Box 64, FIN-00014, Finland*
[c] *Helsinki Polytechnic, Department of Technology, P.O. Box 4020, 00099 Helsinki, Finland*
[d] *College of Oceanic and Atmospheric Sciences, Oregon State University, Corvallis, OR 97331, USA*
[e] *Department of Physics and Astronomy, University College London, London WC1E 6BT, UK*

Received 24 May 2005; received in revised form 30 May 2006; accepted 8 June 2006

Abstract

Analytic and numerical calculations are performed on the production of sulphuric acid aerosol in conditions of a very large nucleation event observed in the upper troposphere. The numerical results feature a growing peak in the size distribution whose magnitude is reproduced well analytically, and are consistent with the observed particle number concentration at sizes greater than 25 nm (measured dry diameter), but suggest that most of the aerosol was at unobserved smaller sizes. Because of growth and coagulation, number concentrations of the aerosol rapidly become independent of the number initially nucleated, so that conclusions as to the nucleation process, either homogeneous or ion-induced nucleation, cannot easily be drawn from existing atmospheric observations. The final concentration is very insensitive to the magnitude of the SO_2 source, but, if condensation on, and coagulation with, a remnant background aerosol occurs, such nucleation events will be cut off for source magnitudes less than a specific value. Anthropogenic emissions of SO_2 which exceed this value can produce higher aerosol number concentrations in the atmosphere with consequences for the indirect effect of aerosols on the climate.

Keywords: Aerosol formation; Nucleation; Sulphuric acid; Nucleation bursts; Atmospheric process

1. Introduction

On May 8, 1996, as part of the SUCCESS study (Toon & Miake-Lye, 1998), a NASA DC8 flew through and near the cirrus outflow of a large midwest storm. An aerosol which was observed with a condensation nucleus counter had maximum concentrations of 12,000 per cm^3 (45,000 in standard units), and extended over a region at least a 600 km in extent (Twohy et al., 2002). This type of atmospheric aerosol production, which resulted from deep convection and is consistent with copious sulphuric acid droplet nucleation in the very cold temperatures of the upper troposphere (Clement, Ford, Twohy, Weinheimer, & Campos, 2002a, hereafter denoted as I), is likely to contribute substantially to the number concentration of the background aerosol in the midlatitude upper troposphere (Twohy et al., 2002), and must therefore be included in climate analyses. In this paper we use analytic and numerical calculations to examine

* Corresponding author. Tel.: +44 20 7679 7136; fax: +44 20 7679 7145.
E-mail address: i.ford@ucl.ac.uk (I.J. Ford).

0021-8502/$ - see front matter © 2006 Elsevier Ltd. All rights reserved.
doi:10.1016/j.jaerosci.2006.06.007

the production process, the characteristics of the aerosol produced, and how the SO_2 source strength would affect its occurrence. The magnitude of this source depends on anthropogenic emissions, and if it is not large enough, such a nucleation event will not occur.

An analysis of the production process of this aerosol was made in I which includes an analytic nucleation burst model (Clement & Ford, 1999), and a simple analytic growth and coagulation model. For the estimated growth time of about 5 h following nucleation, the analysis found the mass concentration of the aerosol to be consistent with that observed, and a number concentration a factor of 5 larger than observations. The validity of the analytic models used and their applicability to the observed aerosol are investigated here by performing numerical calculations of the nucleation, growth and coagulation processes using the AEROFOR sectional model (Pirjola, 1999). We extend the calculations beyond 5 h to model the onset of night when the production rate of sulphuric acid from the oxidation of SO_2 is greatly reduced. The initial acid production rate was taken to be $10^5\,\mathrm{cm}^{-3}\,\mathrm{s}^{-1}$ from an estimated SO_2 concentration of 1 ppb and a measured value of OH concentration (Clement et al., 2002a). In the analytic calculation, the number concentration of the aerosol produced was found to be very insensitive to the rate and the SO_2 concentration (Clement et al., 2002a), but this result did not allow for the presence of remaining background aerosol which would reduce the molecular acid concentration by condensation, and also coagulate with any new aerosol produced. This nucleation cutoff mechanism is investigated here. These results, together with those for nightfall, were not included in a preliminary version of this paper (Clement, Pirjola, Twohy, Ford, & Kulmala, 2002b).

We begin, in Section 2, by describing in some detail the analytic growth and coagulation model of I, the separate growth and coagulation timescales of the model, and the predicted number concentration and size at large times. The approach to this limit is examined closely, and the asymptotic number concentration is put in a different form where its independence of the initial nucleated number concentration is manifest, and a sign error in Eq. (17) of I is corrected. It is also pointed out how the analytic model can be extended to later times through successive periods of constant acid production.

Numerical calculations of number concentrations are described in Section 3 and the results are compared with those of the analytic model and the observations. It becomes apparent that, although a nucleation peak persists in the aerosol size distribution predicted numerically as long as the acid production rate is significant, it is all coagulating with the growing peak predicted alone by the analytic model, so that both calculations ultimately produce essentially the same aerosol. In Section 4 we describe results of calculations of the aerosol size moments to investigate consistency with mass conservation and differences between the numerical and analytic models. In Section 5, we investigate in the numerical model how the presence of background aerosol cuts off the nucleation event by its two effects of removing acid molecules by condensation on it and removing very small growing particles by coagulation. The amount of background aerosol needed to cut off nucleation events is investigated for a wide range of acid production rates.

Finally, in Section 6, we discuss the results obtained and give some far-reaching conclusions regarding the nucleation mechanism in the upper atmosphere, and the need for better observations to determine the frequency of upper troposphere nucleation events and conditions necessary for their initiation.

2. Analytic growth and coagulation model

The analytic and numerical models used in this paper are summarised in Table 1, where P is the sulphuric acid molecular production rate, previously taken to be $10^5\,\mathrm{cm}^{-3}\,\mathrm{s}^{-1}$, the estimated value at the observation time.

Table 1
Comparison of treatments of key processes in the analytic and numerical models

Process	Numerical	Analytic
Nucleation rate	Parametrised model	Parametrised model
Period for nucleation	All times	Initial burst interval
Growth	Calculated from ρ	Proportional to P
Size distribution	Sectional	Monodisperse
Period for coagulation	All times	After burst

P refers to the acid molecular production rate and ρ to the acid vapour concentration.

The analytic model was derived in I, and we examine its properties here to bring out particularly its asymptotic form at long times. For the nucleation rate, we used the parametrisation of Kulmala, Laaksonen, and Pirjola (1998), which at the very low temperature of 215 K describes almost barrierless nucleation, being proportional to the acid vapour concentration, ρ, raised to a power close to 2. There are considerable uncertainties in this model, but calculations indicate that use of a more recent model (Vehkamäki et al., 2002) would not change the results significantly. For the nucleation burst, the analytic model employed an expression, given by Clement and Ford (1999), for the total number N_0 of particles produced, whilst the numerical model had nucleation occurring at all times according to the calculated value of ρ. The analytic growth and coagulation model assumed the size distribution had a monodisperse form with a corresponding coagulation rate in the free molecular regime, so that the equation for the number concentration, N, is

$$\mathrm{d}N/\mathrm{d}t = -\tfrac{1}{2}\, K_0 R^{1/2} N^2, \tag{1}$$

where R is the aerosol radius and the rate constant is generally

$$K_0 = 8(3k_\mathrm{B}T/\rho_\mathrm{d})^{1/2} = 0.4515\, T(K)^{1/2} 10^{-16}\,\mathrm{m^3\,s^{-1}}, \tag{2}$$

where k_B is Boltzmann's constant, the droplet density, ρ_d, is taken as $1.3\,\mathrm{g\,cm^{-3}}$ for sulphuric acid, and the result applies when R in Eq. (1) has its numerical value in nm. The numerical value for K_0 quoted in I applies when $T = 215$ K, but inadvertently had the factor of 10^{-16} missing, although this omission was not made in the actual calculation.

During the growth and coagulation process, a uniform volume transfer rate, G, to the aerosol is assumed in the analytic model:

$$G = d(NR^3)/\mathrm{d}t = (3/4\pi) M_\mathrm{a} \eta P/\rho_\mathrm{d} = g N_0 R_0^3, \tag{3}$$

where N_0 is the initial aerosol number concentration at radius R_0, M_a is the molecular mass, and η is a factor needed to take account of the associated water condensation (see I). This equation defines the growth timescale g^{-1} with the parameter g used previously in I, and, while P remains constant, we have

$$NR^3 = N_0 R_0^3 + Gt. \tag{4}$$

The full solution of Eqs. (1) and (2) was derived in I as

$$N/N_0 = \{1 + [5/(7gt_\mathrm{c})][(1+gt)^{7/6} - 1]\}^{-6/5}, \tag{5}$$

where the coagulation timescale is

$$t_\mathrm{c} = (K_0 R_0^{1/2} N_0/2)^{-1} = 4.4310^{10}/[R_0(\mathrm{nm})^{1/2} T(K)^{1/2} N_0\ (\mathrm{cm^{-3}})]\,\mathrm{s}. \tag{6}$$

The initial values taken from the analytic burst model in I were $N_0 = 7 \times 10^6\,\mathrm{cm^{-3}}$, with $R_0 = 1$ nm, $T = 215$ K, which make $t_\mathrm{c} = 7.2$ min. Note that R_0 is the volume average radius of the aerosol following the nucleation burst (Clement & Ford, 1999), and is not the considerably smaller critical radius of a stable nucleus used in the nucleation theory in the following numerical model.

From Eqs. (3)–(5), the full solution for the aerosol radius is

$$R/R_0 = (1+gt)^{1/3}\{1 + [5/(7gt_\mathrm{c})][(1+gt)^{7/6} - 1]\}^{2/5}, \tag{7}$$

It is instructive to expand the solutions (5) and (7) for small times:

$$N/N_0 \approx 1 - t/t_\mathrm{c}, \tag{8a}$$

$$R/R_0 \approx 1 + (1/3)(gt + t/t_\mathrm{c}). \tag{8b}$$

Coagulation is not affected by growth to this order and the dominant increase in R arises from the mechanism with the smaller timescale. The initial growth timescale in I was $g^{-1} = 14.05$ min, so that the aerosol rapidly grows out of the region where a small t expansion is valid.

We now wish to examine closely the asymptotic form for N/N_0 which was used in I and is obtained from Eq. (5) at large times. For $gt \gg 1$, expression (5) can be expanded to give

$$N/N_0 = [1 + (5/7)(gt)^{1/6}(t/t_\mathrm{c})]^{-6/5}. \tag{9}$$

From Eq. (3), we see that this expansion is valid if

$$Gt/(N_0 R_0^3) \gg 1, \tag{10}$$

i.e. the accumulated volume of the aerosol is much larger than the volume at nucleation. This is likely to be satisfied after a relatively short time if the nucleation process is terminated by the lowering of the vapour concentration by growth of the newly nucleated aerosol. It is amply satisfied after an hour following the nucleation burst model used in I. For further expansion, we need the second term in the bracket in (9) to be much greater than 1, which, as $(gt)^{1/6}$ is not large, requires that $t \gg t_c$. With the above value of $t_c = 7.3$ min, this is again satisfied after an hour for the situation described in I. Altogether, we can see from the forms of (5) and (9) that, if it turns out that $N \ll N_0$, then N must have taken on its asymptotic form. This form is that derived in I (Eqs. (A4), (16), and (17)), but not in the following better form:

$$N = (2.8/K_0)^{6/5} t^{-7/5} G^{-1/5}. \tag{11}$$

In I, the form given by Eq. (17) erroneously has $(2.8/K_0)^{-6/5}$ as the first factor.

The important point, not brought out in I, is that this number concentration is independent of the nucleation variables, N_0 and R_0, and thus of the nucleation process itself. In this way, it is analogous to the well-known result for the coagulation of an aerosol at a constant rate, K, where

$$\mathrm{d}N/\mathrm{d}t = -\tfrac{1}{2} K N^2, \tag{12}$$

whose solution is

$$N = N_0/(1 + \tfrac{1}{2} N_0 K t) \sim 2/(Kt), \quad t \to \infty. \tag{13}$$

If the actual aerosol size distribution behaves as predicted by this monodisperse model, the number concentration becomes independent of the nucleation process. Application of this result to atmospheric aerosols is discussed in Section 4.

From Eqs. (4) and (11) we obtain the asymptotic aerosol radius at constant P as

$$R = (2.8/K_0)^{-2/5} G^{2/5} t^{4/5} = 3.647 P^{2/5} (10^5\ \mathrm{cm^{-3}\ s^{-1}}) t^{4/5} (h)\ \mathrm{nm}, \tag{14}$$

where the numerical result is normalised to the upper troposphere conditions of the aerosol formation described in I with $P = 10^5\ \mathrm{cm^{-3}\ s^{-1}}$.

The initial observed burst took place at about 10 a.m. local time (see I) and observations were made after about 5 h at about 3 p.m., and calculations in I were made for this 5 h period. To continue the analytic model after nightfall at about 5 p.m., we assume that the production rate, P, and thus growth rate, G, are reduced by a factor of 100 at this time (7 h after the burst), and for later times again use Eq. (5) with N_0 ($t = 0$) replaced by N ($t = 7$ h), and g in Eq. (3) and t_c in Eq. (6) specified by N and R at $t = 7$ h. When the substitutions are made with N (7 h) $= 38862\ \mathrm{cm^{-3}}$ and R (7 h) $= 17.72$ nm, we find the timescales increased to $t_c = 5.13$ h and $g^{-1} = 723$ h. This means that the small time expansions (8) are valid for an hour or two after the reduction in P and changes to the aerosol are dominated by coagulation. We cannot use approximation (11) in the second region. Instead, gt is always small in the region of our calculation up to a total time of 20 h, so that we can expand (5) and (7) to give the coagulation solutions as good approximations:

$$N/N_0 = [1 + \tfrac{5}{6}(t/t_c)]^{-6/5}, \tag{15a}$$

$$R/R_0 = [1 + \tfrac{5}{6}(t/t_c)]^{2/5}. \tag{15b}$$

We can find asymptotic expansions for large t/t_c from Eq. (6) for t_c, but these now depend on N_0 and R_0; for example, N has the weak dependence as $N_0^{-0.2}\ R_0^{-0.6}$. However, these parameters, and the results (15), do not depend on their values after the initial nucleation burst if, as in our case, the asymptotic form (11) is valid later in the first time period.

This process can be extended to obtain an analytic form for N after any number of time periods in which the molecular production rate, P, and thus the volume production rate, G, are constant. We emphasise the crucial point that the condition for losing memory of the initial nucleation burst is that, for any time period, $t \gg g^{-1}$ and t_c.

3. Numerical calculations

The numerical calculations used a sectional model with 54 sections for a sulphuric acid aerosol (Pirjola, 1999). In contrast to the analytic model, the numerical model had a full sectional size distribution and coagulation rate, and condensation on the aerosol was calculated from the evolving molecular acid concentration, ρ. Calculations were made in the numerical model with the same abrupt drop at 5 p.m. by a factor of 100 in P, but we also performed calculations with the more realistic assumption of a semisinusoidal form for P (sine function of time during daylight hours), peaking at $10^5\ \mathrm{cm}^{-3}\ \mathrm{s}^{-1}$ at midday, and reducing to $P/100$ for times after 5 p.m. A reasonable estimate for the acid production rate in the event observed is $P = 10^5\ \mathrm{cm}^{-3}\ \mathrm{s}^{-1}$ (see I), but we have also performed calculations for values larger and smaller by a factor of 10. The results are now compared to those from the analytic model.

The results of the numerical calculations all have similar features, and in Fig. 1 we show aerosol and acid number concentrations as functions of time (upper frame) and particle size distributions at different times (lower frame). These are for the calculated ambient wet aerosol, whereas the observations were made after drying the aerosol. Both the acid vapour concentration and the total number of particles have sharp peaks at short times under an hour during which a very large number of particles are nucleated. The peaks soon subside as condensation increases on the nucleated aerosol, and the concentration and N_{tot} then decrease slowly with time. The size distribution initially just has a nucleation peak (see 21 min), develops a growing shoulder at larger sizes by 1 h, and by 2 h, has clearly separated into two parts, a growing peak and a separate nucleation peak at very small sizes. The minimum between the peaks arises from coagulation of the nucleation peak with the growing peak, a mechanism which effectively cuts off nucleation of particles which

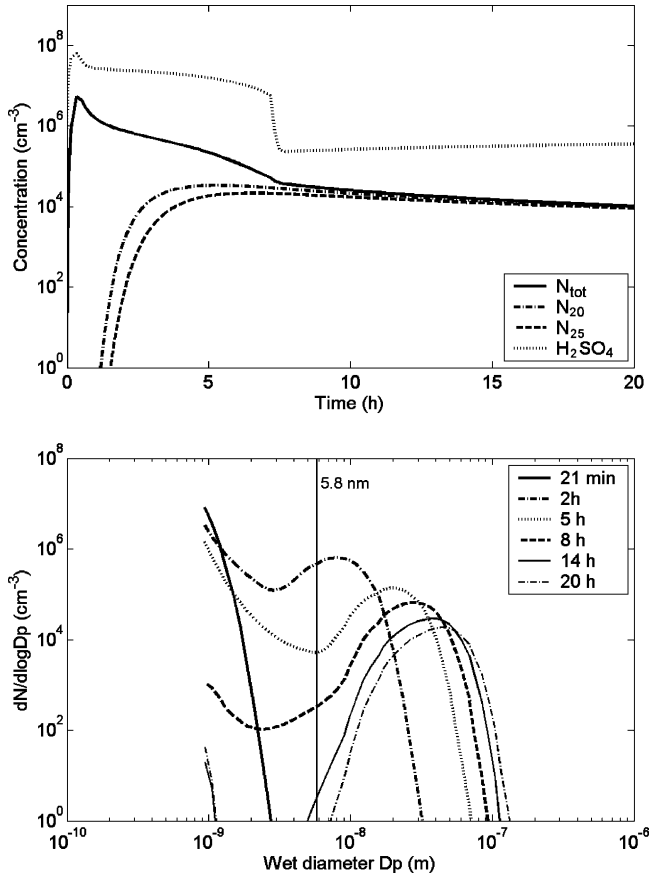

Fig. 1. Concentrations calculated numerically as functions of time for molecular sulphuric acid (H_2SO_4), total aerosol number (N_{tot}), and aerosol numbers with diameters over 20 nm (N_{20}) and 25 nm (N_{25}). In the lower frame, aerosol size distributions as functions of diameter (D_{p}) are shown at 6 times, and the minimum between the growing peak and nucleation peak is indicated at 5 h.

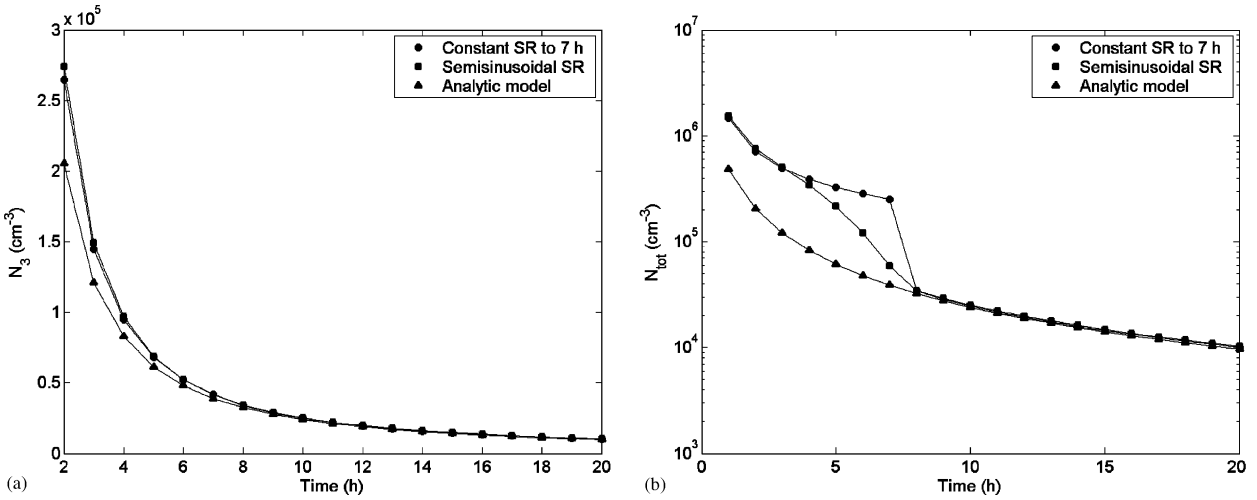

Fig. 2. Aerosol number concentrations, N, as functions of time calculated numerically and by the analytic model. In (a) the numerical result is for particles with diameters over 3 nm calculated with the semisinusoidal source rate up to 7 h and in (b) the numerical results are for total concentrations at all sizes with constant and semisinusoidal source rates up to 7 h (as in Fig. 1).

Table 2
Variation of predicted number concentrations and particle radius, R, after 5 h with molecular acid production rate, P

P ($cm^{-3}\,s^{-1}$)	N_3 (numerical) cm^{-3}	N (analytic) cm^{-3}	Error[a] (%)	N_{25} (numerical) cm^{-3}	R (nm)
10^4	1.20×10^5	1.03×10^5	−14	0.49×10^4	5.26
10^5	6.71×10^4	6.48×10^4	−3	1.82×10^4	13.22
10^6	4.23×10^4	4.09×10^4	−3	4.19×10^4	33.21

[a]Deviation of N (analytic) from N (numerical).

survive to grow to large size. The nucleation peak contains more particles and remains as long as the acid production and concentration remain high, but becomes insignificant when the production is reduced by nightfall. All these tiny particles are coagulating with the growing peak, and their population rapidly falls when molecular acid production ceases.

Essentially all the acid mass produced is transferred to the growing peak, some of it by direct condensation and the rest via coagulation with the nucleation peak. This is the main reason why there is good agreement, even at relatively short times, between the number concentration in the growing peak in the numerical model and that predicted by the analytic model in which nucleation has ceased. This is shown in Fig. 2a by a comparison between the analytic result and that predicted by the numerical model with the semisinusoidal production rate, for which the number concentration in the growing peak is approximated by the area under the distribution for diameters greater than 3 nm. The analytic model predicts that a radius of 3 nm is reached in approximately 37 min after the nucleation burst. In Fig. 2b we compare total aerosol number concentrations predicted analytically and by the numerical models for semisinusoidal and constant production rates up to 7 h. The differences between them practically disappear at later times when acid production is reduced. The large difference in N_{tot} between the numerical and analytic models for times up to 7 h shown in Fig. 2b contrasts with the closeness of N_3 in Fig. 2a and shows that the dominant contribution to N_{tot} in this region arises from tiny particles below 3 nm in size.

A similar agreement applies for the lower and higher values of P, and the detailed number concentrations after 5 h are compared in Table 2, where we also show the radii of the analytic monodisperse aerosol predicted by Eq. (14) in the analytic model. The numerical concentration, N_3, is that for particles over 3 nm in diameter calculated with a critical nucleation radius of 0.4 nm and a constant production rate, P. Choice of this radius up to 0.5 nm can produce variations in N_3 (5 h) of about 20%. However, it is clear that, in a timescale of hours, the asymptotic analytic form (11) can provide accurate predictions of total aerosol number concentrations reached by this type of atmospheric aerosol

Table 3
Condensation nuclei counter efficiencies

Diameter (nm)	10	12	16	20	30	40	50	60	70
Efficiency (%)	1	3	14	30	54	70	84	97	100

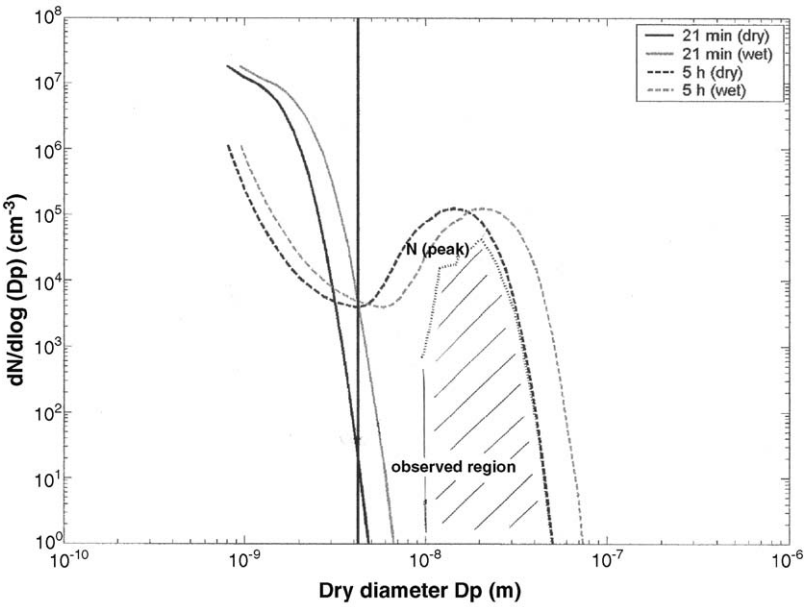

Fig. 3. Aerosol size distributions calculated for wet and dry conditions after 5 h with the observed size region indicated. The number of particles, N (peak), in the size region to the right of the vertical line from the minimum, is very close to the predicted analytic value (see Table 2).

formation. Furthermore, the number concentration is independent of the initial number of particles nucleated, and varies only with the mass transfer rate to the aerosol which is determined by the acid production rate. This conclusion has important consequences for the observation and interpretation of atmospheric aerosol formation events that we discuss in Section 5. To discuss the observability of the aerosol produced (see below), we also give in Table 2 the concentration, N_{25}, for particles over 25 nm in diameter.

The origin of the weak inverse dependence, proportional to $P^{-1/5}$, of the total aerosol number concentration produced in a given time is the increase in the coagulation rate with size which is proportional to $R^{1/2}$. This increase only applies for small particles for which coagulation is in the free molecular regime. We discuss the limitation arising from growth out of this regime in Section 4, where we also discuss the influence of background aerosol on the nucleation process.

For the atmospheric aerosol observed by Twohy et al. (2002), the case considered in I, the analytic value of N is $6.48 \times 10^4\ \mathrm{cm}^{-3}$ at $t = 5$ h, which is about 5 times the observed value. The measured value of the number concentration was $1.2 \times 10^4\ \mathrm{cm}^{-3}$ with a quoted efficiency of 50–90% across the size range of dry (measured) diameters greater than 25 nm. Predicted numerical number concentrations after 5 h are much bigger, $6.71 \times 10^4\ \mathrm{cm}^{-3}$ for the semisinusoidal case above 3 nm, but much of the distribution is less than 25 nm in diameter (predicted $N_{25} = 1.82 \times 10^4\ \mathrm{cm}^{-3}$ in Table 2), suggesting that most of it was unobserved. To examine this possibility quantitatively, we have taken the quoted efficiencies for the CN counter at 200 mb (Zhang & Liu, 1991) reproduced in Table 3 to produce a numerical size distribution modified by observation efficiencies. This is shown in Fig. 3 where the hatched area represents the actual predicted total observable number concentration which we find to be $1.39 \times 10^4\ \mathrm{cm}^{-3}$. Predicted values of $N(> 25\ \mathrm{nm})$ range from $1.02 \times 10^4\ \mathrm{cm}^{-3}$ to $2.09 \times 10^4\ \mathrm{cm}^{-3}$ for constant and semisinusoidal source rates so that the difference of about 16% between the predicted and observed values is well within uncertainties in the calculations. As we surmised in I, the numerical calculations suggest that much of the aerosol was not observed, and the predicted and observed concentrations are now in agreement under their respective uncertainty ranges. To check on the present consistency

between observation and theory, it is important that future observations are able to measure smaller sizes of this type of aerosol.

4. Mass conservation and aerosol size

Moments of the numerical aerosol size distribution are defined by

$$M_n = \int R^n n(R)\,\mathrm{d}R, \tag{16}$$

where the total number concentration, N, is given by the zeroth moment.

Corresponding mean radii related to these moments may be defined by

$$\langle R_n \rangle = (M_n/N)^{1/n}. \tag{17}$$

The third moment gives the total volume concentration of the aerosol and is thus related to the mass concentration, M, of the aerosol,

$$M = (4\pi/3) M_3 \rho_\mathrm{d} = (4\pi/3)\rho_\mathrm{d} N \langle R_3 \rangle^3, \tag{18}$$

where ρ_d is the density of liquid in the droplets.

If there is no initial sulphuric acid in the atmosphere, and the final molecular acid concentration is c, mass conservation relates the total molecular acid production at a rate $P(t)$ to the sum of the mass concentrations in the aerosol and in the atmosphere:

$$M_\mathrm{a} \int P(t)\,\mathrm{d}t = M/\eta + M_\mathrm{a} c, \tag{19}$$

where M_a is the molecular mass and η is the factor relating the aerosol mass including water to the acid mass in the aerosol.

In the numerical calculations, the integral in M_3 is divided into two parts with a cutoff between the nucleation peak and the growing peak. After a relatively short time the contribution to M_3 of the nucleation peak should be negligible, and can be neglected in (19). Also, we can obtain the mass in the atmosphere from calculated values of c. With the neglect of these two corrections, we can then relate the aerosol size from the third moment of the growing size distribution (above the cutoff radius):

$$\langle R_3 \rangle^3 = (3/4\pi) M_\mathrm{a} \eta/(N \rho_\mathrm{d}) \int P(t)\,\mathrm{d}t. \tag{20}$$

Values of $\langle R_3 \rangle$ obtained from the cutoff integral and from the integral over the production rate are compared in Fig. 4. Their close agreement verifies the validity of neglecting the two corrections as well as that the overall numerical program conserves mass.

As the basic premise of the analytic model is that all acid production condenses on the aerosol, Eq. (20) is automatically satisfied, and, with the same production rate and initial mass, the predicted radius, R, should also agree with $\langle R_3 \rangle$ from the numerical model. However, differences can arise from the sinusoidal form of $P(t)$ used in the numerical model and the initial volume, $N_0 R_0^3$, of the analytic model, whereas there is no initial aerosol at $t = 0$ in the numerical case. Moments calculated as functions of time for the two models are compared in Fig. 5 which includes results calculated with a constant source rate by the monodisperse numerical model (Pirjola & Kulmala, 2000; Pirjola, Tsyro, Tarrason, & Kulmala, 2003). Values of R are somewhat larger than values of $\langle R_3 \rangle$ from the numerical model with the semisinusoidal source rate, but agree very well with monodisperse values, R_mon, with the constant source rate up to 7 h, showing the consistency with mass conservation and the basic assumption of the numerical model.

Values from the lower moments, $\langle R_1 \rangle$ and $\langle R_2 \rangle$, are smaller than $\langle R_3 \rangle$ and substantially below the analytic values for R. As these moments govern the condensation rate on the aerosol, it might be thought that condensation rates would be smaller in the numerical calculation. This is not the case: with a lower condensation sink, the atmospheric acid concentration increases and transfer via coagulation with small nucleated particles increases to make the total mass transfers identical. Apart from a very short initial time period lasting less than 1 h, the mass transfer rate to the growing

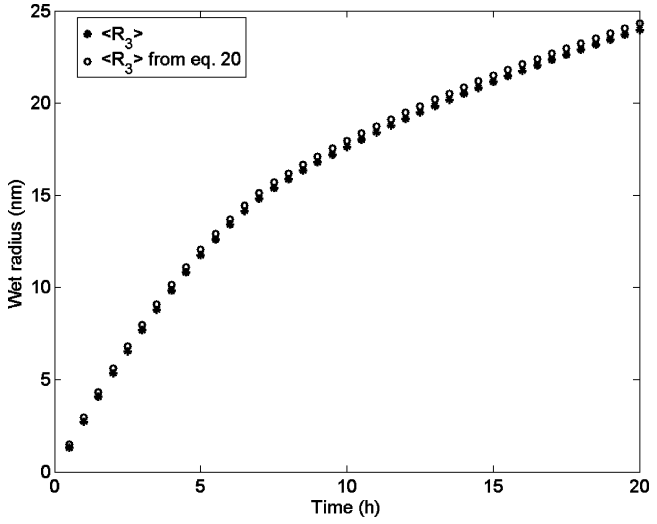

Fig. 4. Values of $\langle R_3 \rangle$ obtained from a cutoff integral over the size distribution and from the integral over the production rate (Eq. (20)) as functions of time.

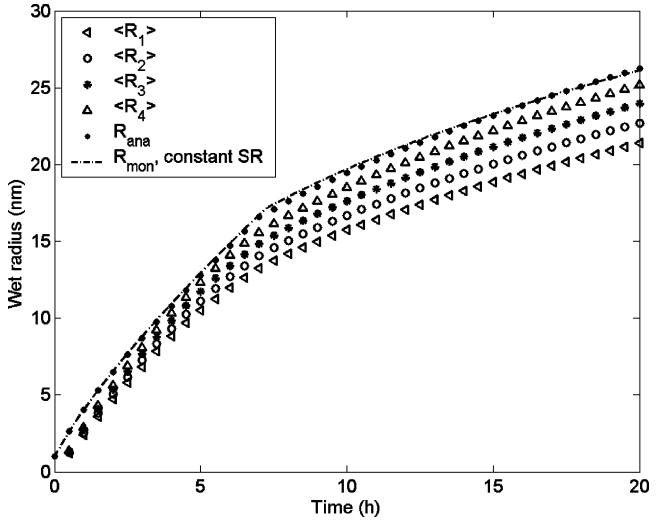

Fig. 5. Wet radii $\langle R_n \rangle$ from moments of the size distribution compared to radii from the analytic and monodisperse numerical models for the time period to 20 h.

aerosol is specified solely by the production rate, P, and this is clearly evident in all the results from the numerical model.

The amount of water present, and its relative humidity (RH), can strongly affect the initial aerosol nucleation process, but, as long as a nucleation event occurs, it does not affect strongly the subsequent evolution and growth of the aerosol. Acid transfer to the aerosol is fixed as we have just seen. Water transfer enters through the proportionality of the growth rate, G, to the parameter $\eta\rho_d$ as well as to P (see Eq. (3)). In the initial asymptotic region the number concentration (Eq. (11)) and radius (Eq. (14)) are thus proportional to $(\eta/\rho_d)^{-1/5}$ and $(\eta/\rho_d)^{2/5}$, respectively. In the original calculation (Clement et al., 2002a) we used $\eta^{-1} = 0.36$ and $\rho_d = 1.3\,\mathrm{g\,cm^{-3}}$ which corresponds to 50 ppm of water and RH of 40% at $T = 215$ K. These figures may not be accurate, and indeed during the growth period of many hours the humidity could change significantly, but changes to η and ρ_d are very unlikely to change N and R significantly.

5. Model limitations and nucleation cutoff

The analytic model has important limitations mainly arising from the possible presence of background aerosol. The numerical calculations confirm its prediction that final number concentrations are very insensitive to the source rate, P, but we do not expect actual formation of a new aerosol if P is sufficiently small. Realistically, however, nucleation events will not occur if there is sufficient background aerosol left, after cleansing by a storm, to condense the acid molecules and to coagulate with the newly nucleated aerosol. We have performed calculations to illustrate this effect by introducing a background aerosol of number concentration N_{bg} and radius R_{B} into the numerical calculations. The rate of change $\mathrm{d}\rho/\mathrm{d}t$ of the acid molecular concentration ρ then has an additional loss term, $-\Lambda_{\mathrm{cond}}\rho$, where

$$\Lambda_{\mathrm{cond}} = C(\mathrm{cond})N_{\mathrm{bg}}\beta_{\mathrm{B}}(R_{\mathrm{B}}), \tag{21}$$

where $C(\mathrm{cond})$ is a constant and β is the Fuchs–Sutugin factor. This factor causes Λ to change from a proportionality to R_{B}^2 (surface area) at small R_{B} to a proportionality to R_{B} at large sizes where condensation is limited by diffusion and $\beta = 1$.

The rate of change $\mathrm{d}N/\mathrm{d}t$ of the nucleated aerosol number concentration N has a loss term, $\Lambda_{\mathrm{coag}}N$, where

$$\Lambda_{\mathrm{coag}} = C(\mathrm{coag})N_{\mathrm{bg}}R_{\mathrm{B}}/R^2, \tag{22}$$

where $C(\mathrm{coag})$ is another constant and we have quoted the approximate dependence of the coagulation kernel on the typical radius R of the nucleated component and the background aerosol radius R_{B}, for $R_{\mathrm{B}} \gg R$ used by Kerminen and Kulmala (2002). In the numerical calculations no approximations were made to the kernel.

Values of N_{tot} ($t = 5$ h) were obtained for fixed R_{B} as a function of the background number concentration, N_{bg}, and typical results for $R_{\mathrm{B}} = 50$ nm are shown in Fig. 6 for the increase in the number concentration, $N_{\mathrm{tot}} - N_{\mathrm{bg}}$. If the source rate (SR $= P$) is small, e.g. $10^4\,\mathrm{cm}^{-3}\,\mathrm{s}^{-1}$ as shown, very little background aerosol (less than $10^3\,\mathrm{cm}^{-3}$) is needed to suppress the nucleation event completely. For the postulated observed rate of $10^5\,\mathrm{cm}^{-3}\,\mathrm{s}^{-1}$, a few thousand particles per cm^3 would be needed to prevent formation of new particles. Typical background values in the upper stratosphere are of order 1100 std cm^{-3}, or about 300 actual cm^{-3} (Twohy et al., 2002); however, the number concentration present in detraining regions of deep convective storms is not well documented. For higher values of P, larger concentrations of background aerosol would be needed to suppress nucleation, but these are often present in other parts of the atmosphere nearer the ground. Precise amounts of aerosol remaining after storms have to be specified to determine the threshold

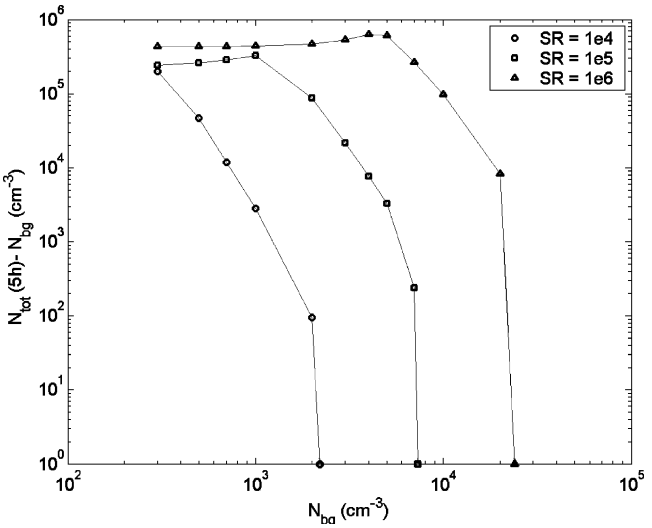

Fig. 6. Total number concentrations after 5 h (N_{tot}) less the initial background concentrations (N_{bg}) calculated numerically for three acid production source rates (SR) in units of $\mathrm{cm}^{-3}\,\mathrm{s}^{-1}$ as functions of N_{bg} of aerosol of radius 50 nm.

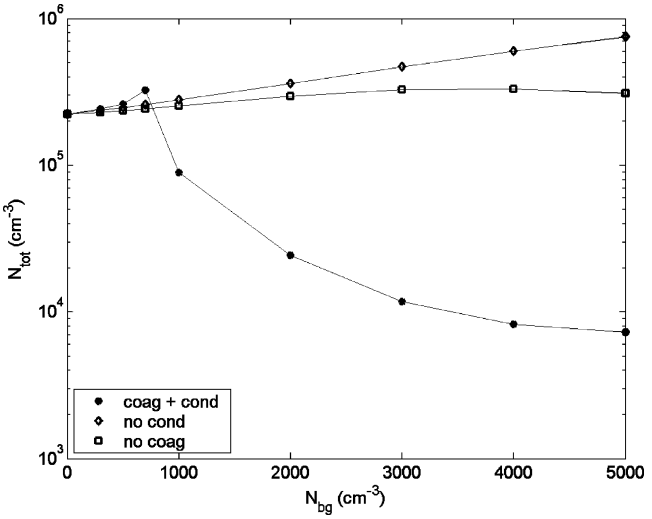

Fig. 7. Total number concentrations after 5 h, N_{tot} (final), calculated for an acid production rate of $10^5\,\mathrm{cm}^{-3}\,\mathrm{s}^{-1}$ in the presence of an initial background aerosol, radius 200 nm, of concentration N_{bg} for three different conditions. In the full calculation coagulation of new aerosol takes place with the background aerosol and molecular condensation of sulphuric acid occurs on it, and the other results show the effect of suppressing each of these removal mechanisms in turn.

precursor source for nucleation events to occur. In Fig. 7, we show typical results that indicate that both loss rates (21) and (22) are required for suppression to occur and they are of equal importance. Without the loss of molecules by condensation onto the background aerosol, the new particles grow fast enough through the very small size region important for coagulation so that nucleation events will occur.

To summarise the above discussion, the importance of the cutoff mechanism is that only high enough concentrations of SO_2 resulting from production rates of over $10^4\,\mathrm{cm}^{-3}\,\mathrm{s}^{-1}$ will lead to the type of enormous nucleation event observed in the SUCCESS project (Twohy et al., 2002). Anthropogenic emissions of the gas near the ground, which are lofted in deep convective storms, can then play a significant role in producing large increases in the number concentration of aerosols in the atmosphere. The number concentrations rise due to increased numbers and sizes of nucleation events rather than increased numbers of particles per event.

For the cases we have discussed in detail, there is an excellent correspondence between the number of nucleated growing aerosol predicted by the analytic model and by the numerical calculations. The results of the analytic model rely on the particle size remaining in the free molecule region for the coagulation rate, and this could limit the correspondence if large sizes are reached during the growth and coagulation process. For the upper troposphere conditions, the free molecule coagulation kernel for equal sized aerosol is an excellent approximation to the actual kernel for particle radii up to $R = 15$ nm (K_{FM} larger by 4.2%). The overestimate with K_{FM} then increases gradually to 14.6% at $R = 25$ nm and 30.8% at $R = 35$ nm, approximately where the actual kernel reaches a maximum. In this region, the overestimation of coagulation by the monodisperse free molecular kernel is partly counteracted by the actual kernel being larger on the average for $R_1 \neq R_2$ than its value for $R_1 = R_2$; for $R_1 = R + \delta$ and $R_2 = R - \delta$ the increase is by a factor of $1 + 3\delta^2/R^2$. Thus, we expect N to be given accurately by the analytic model for sizes up to about 30 nm, and this appears to be borne out by the result for $P = 10^6\,\mathrm{cm}^{-3}\,\mathrm{s}^{-1}$ in Table 2. Above this size, the actual kernel starts to decrease with size, whereas the free molecule form continues to increase, so that we would expect the analytic value of N to underestimate its actual value for particle diameters greater than 70 nm. Eq. (5) or its approximate versions discussed in Section 2 can be used to find when this occurs. For the observations analysed in I, we estimated that the initial SO_2 concentration was 1 ppb which, for continuous uninterrupted conversion to sulphuric acid, would lead to just over 20 h growth and a final size of $R = 41$ nm. This number would be slightly changed by an intervening night of coagulation but little growth, but, judging by the result shown in Fig. 2a there is likely to be little difference in the end between the final analytic and numerical concentrations. On the other hand, at values of P an order of magnitude larger, or SO_2 concentrations of 10 ppb, final sizes would be in the region of 100 nm where a considerable difference might arise.

6. Discussion and conclusions

The comparison between analytic and numerical calculations for this type of near-barrierless nucleation is very illuminating. The simple analytic model predicts the number concentration of growing aerosol quite well at early times in spite of cutting off nucleation early when it actually continues at a significant rate. The tiny nuclei being produced at later times all coagulate with the growing peak of the size distribution, and this is an important means of transferring condensed acid mass to the aerosol. At later times the correspondence between the two number concentrations is excellent, which is not surprising as we have shown that the number concentration in the analytic model becomes completely independent of the nucleation process. As far as the aerosol number concentration is concerned, the analytic model reproduces the effects of growth and coagulation in the free molecule region as well as the full sectional model.

The predicted aerosol size differs slightly between the models, firstly from the lower acid mass produced by the semisinusoidal source rate used in the numerical model, and secondly according to the radius moment used in the numerical case. The numerical model supports the basic premise of the analytic model in that practically all the acid production is condensed on the growing aerosol, and is itself internally consistent in satisfying mass conservation. Radii from moments of the numerical size distribution lower than the third mass moment are smaller than the value of the analytic radius, but this does not mean that condensation on the aerosol, the rate of which is governed by the first and second moments, is smaller than in the analytic case.

The theory based on first principles, with only the condensation of sulphuric acid and water, now predicts an atmospheric number concentration for the case considered in I consistent with the observed value (Twohy et al., 2002). Only a fraction of the aerosol was probably seen as there were many more particles at smaller unobserved sizes. However, the aerosol was well into the concentration and size region where any characteristic dependence on nucleation mechanism had vanished. Thus the agreement does not tell us anything about the nucleation mechanism, but only that an event occurred. The conclusion in I that the result supports the binary homogeneous nucleation mechanism is unjustified, since other mechanisms could produce essentially the same results.

It is likely that exactly similar conclusions apply to the results reported by Lee et al. (2003) based on calculations of ion-induced nucleation using the theory of Lovejoy, Curtius, and Froyd (2004). The apparent very good agreement, especially at later times (their Fig. 2b), between predictions of the model and observed aerosol size distribution at high altitude probably arises just from reproducing the correct acid production rate and correctly describing aerosol growth and coagulation. Also, as Lee et al. (2003) themselves remark, their calculations of the very small (up to about 9 nm) particles at the low acid production rate of $P = 300\,\mathrm{cm}^{-3}\,\mathrm{s}^{-1}$ are very sensitive to the amount of background aerosol present (as would be predicted from our Fig. 6), and they do not rule out the possibility of homogeneous nucleation. Our conclusion is that there is presently not enough observational evidence to decide which of homogeneous nucleation and ion-induced nucleation is the dominant mechanism in the upper troposphere and lower stratosphere, a point we now examine in more detail.

It is very likely that no other nucleation mechanism could be involved; significant ternary nucleation involving ammonia would require the air mass emerging from the storm (Twohy et al., 2002) to contain unreasonably large ammonia concentrations. The nature of the dominant mechanism will depend on the closeness of the binary sulphuric acid–water nucleation rate to its kinetic or barrierless limit. At this limit, ion-induced nucleation is ruled out because ion concentrations are always much smaller than those of neutral molecules, and the homogeneous nucleation rate is just given by the square of the neutral acid concentration times a kinetic factor. Any enhancement from electric fields in the kinetic factor multiplying charged ion concentrations in the corresponding ion-induced rate will not be large enough to overcome the disparity in the concentrations. Parametrised homogeneous rates (Kulmala et al., 1998; Vehkamäki et al., 2002) are of the order of a factor 50 smaller than the barrierless rate at the cold upper troposphere conditions that we consider here, which may be close enough to make homogeneous nucleation dominant. However, there is not enough experimental information on the stability of neutral clusters at these temperatures to reach a firm conclusion. There is a strong incentive to make improved measurements at early times of nucleation events in the upper troposphere where differences between the mechanisms will be more apparent.

The calculations show that nucleation events will be cut off when a background aerosol is present with number concentration above a sharp threshold (see Fig. 6). This threshold is low for small acid source rates and SO_2 concentrations, but increases to a large value, which would not be expected from air cleaning after emerging from a storm, at high source rates of $P = 10^5\,\mathrm{cm}^{-3}\,\mathrm{s}^{-1}$ or greater. The subject needs to be studied further to obtain more precise values for aerosol emerging from storms, and measurements are needed of SO_2 and acid concentrations in the corresponding outflows.

There is an obvious potential for increased anthropogenic or other emissions of SO_2 to produce more of the large upper troposphere nucleation events. Extensive measurements over the Pacific have shown that the small particles produced in such events age and subside to form cloud condensation nuclei (CCN) when mixed into the marine boundary layer (Clarke & Kapustin, 2002). An increase in the frequency of upper troposphere nucleation events from an increase in SO_2 sources has the potential to affect the climate, due to changes in cloud properties resulting from the consequent increase in CCN.

Estimates (Twohy et al., 2002) have already shown that nucleation from deep convective events may contribute significantly to atmospheric aerosol in midlatitudes. Adams and Seinfeld (2003) have suggested that direct particle emissions make a greater contribution to global CCN concentrations than nucleation events driven by SO_2 emissions. However, our work demonstrates that the impact of such events depends on the SO_2 source strength and the concentration of pre-existing aerosol after storms. Until major nucleation events in the atmosphere are better quantified in terms of frequency and outcome, current global models may be inadequate to specify the origins of the atmospheric number concentrations of CCN.

In terms of climate impact, our work has shown that new aerosol number concentrations from a deep convective nucleation event do not depend on the nucleation mechanism, are insensitive to the amount of acid produced, and that their number and size are accurately given by a simple model. The frequency of such events then becomes the main unresolved issue, and this is strongly influenced by the acid production rate, the amount of background aerosol present, and, in contrast to the final aerosol, will be affected by the nature of the nucleation mechanism.

References

Adams, P. J., & Seinfeld, J. H. (2003). Disproportionate impact of particulate emissions on global cloud condensation nuclei concentrations. *Geophysical Research Letters*, *30*, 1239.

Clarke, A. D., & Kapustin, V. N. (2002). A Pacific Aerosol Survey. Part I: A decade of data on particle production, transport, evolution, and mixing in the troposphere. *Journal of Atmospheric Science*, *59*, 363–382.

Clement, C. F., & Ford, I. J. (1999). Gas-to-particle conversion in the atmosphere: II. Analytical models of nucleation bursts. *Atmospheric Environment*, *33*, 489–499.

Clement, C. F., Ford, I. J., Twohy, C. H., Weinheimer, A., & Campos, T. (2002a). Particle production in the outflow of a mid-latitude storm. *Journal of Geophysical Research*, *107*(D21), 4559.

Clement, C. F., Pirjola, L., Twohy, C. H., Ford, I. J., & Kulmala, M. (2002b). Analytic and numerical calculations of formation of a sulphuric acid aerosol in the upper troposphere. In C.-S. Wang (Ed.), *Proceedings of the sixth international aerosol conference* (Vol 1, pp. 271–272), Taipei, Taiwan.

Kerminen, V.-M., & Kulmala, M. (2002). Analytic formulae connecting the "real" and the "apparent" nucleation rate and the nuclei number concentration for atmospheric nucleation events. *Journal of Aerosol Science*, *33*, 609–622.

Kulmala, M., Laaksonen, A., & Pirjola, L. (1998). Parametrization for sulfuric acid/water nucleation rates. *Journal of Geophysical Research*, *103*(D7), 88301–88307.

Lee, S.-H., Reeves, J. M., Wilson, J. C., Hunton, D. E., Viggiano, A. A., Miller, T. M. et al. (2003). Particle formation by ion nucleation in the upper stratosphere and lower troposphere. *Science*, *301*, 1886–1889.

Lovejoy, E. R., Curtius, J., & Froyd, K. D. (2004). Atmospheric ion-induced nucleation of sulfuric acid and water. *Journal of Geophysical Research*, *109*, D08204.

Pirjola, L. (1999). Effects of the increased UV radiation and biogenic VOC emissions on ultrafine sulphate aerosol formation. *Journal of Aerosol Science*, *30*, 355–367.

Pirjola, L., & Kulmala, M. (2000). Aerosol dynamical model MULTIMONO. *Boreal Environment Research*, *5*, 361–374.

Pirjola, L., Tsyro, S., Tarrason, L., & Kulmala, M. (2003). A monodisperse aerodynamics module: A promising candidate for use in the Eulerian long-range transport model. *Journal of Geophysical Research*, *108*(D9), 4258.

Toon, O. B., & Miake-Lye, R. C. (1998). Subsonic aircraft: Contrail and cloud effects special study (SUCCESS). *Geophysical Research Letters*, *25*, 1109–1112.

Twohy, C. H., Clement, C. F., Gandrud, B. W., Weinheimer, A. J., Campos, T. L., Baumgardner, D. et al. (2002). Deep convection as a source of new particles in the midlatitude upper troposphere. *Journal of Geophysical Research*, *107*(D21), 4560.

Vehkamäki, H., Kulmala, M., Napari, I., Lehtinen, K. E. J., Timmreck, C., Noppel, M. et al. (2002). An improved parametrization for sulfuric acid-water nucleation rates for tropospheric and stratospheric conditions. *Journal of Geophysical Research*, *107*(D22), 4622.

Zhang, Z., & Liu, B. Y. H. (1991). Performance of TSI 3760 condensation nuclei counter at reduced pressure and flow rates. *Aerosol Science and Technology*, *15*, 228–238.